Design Optimization for 4.1-THZ Quantum Cascade Lasers

F. Esmailifard*, M. K. Moravvej-Farshi* and K. Saghafi**

Abstract: We present an optimized design for GaAs/AlGaAs quantum cascade lasers operating at 4.1THz. This was based on a three-well active module with diagonal radiative transition. This was performed by modifying the existing model structure, to reduce the parasitic anticrossings (leakage currents) as well as the optical gain linewidth. While the gain FWHM was reduced by more than 50% the gain peak was increased by about 23.3%.

Keywords: Quantum Cascade Laser, Resonant Tunneling Transport, Parasitic Current Channel.

1 Introduction

A challenge associated with terahertz-quantum cascade lasers (THz-QCLs) is to achieve population inversion in a THz inter-subband structure, at room temperature. Due to the small subband energy separation, thermal excitation of electrons from the ground state into the lower laser state reduces the population inversion between the laser states. Among recently reported successful designs, based on a three-well module incorporated with depopulation process assisted by coherent resonant-tunneling (CRT) [1-4], pulsed mode operation of THz-QCLs up to a heat-sink temperature of 186 K is noticeable [2]. This performance was achieved by an inter-well (diagonal) radiation design that has limited the flow of parasitic leakage current, which in turn has decreased the operating current density.

In this letter, by modifying the diagonal design of [2], we have achieved an optimized design for a THz-QCL, with reduced parasitic current channels, increased oscillator strength (dipole matrix element, z_{43}), and a decreased radiative transition linewidth, all of which have provided an improved optical gain.

2 Design Procedure

A major goal, in THz-QCL design, is to minimize injection of carriers into lower energy subbands for the applied fields below the design bias. It is well-known that these carriers, which result in parasitic current channels, can undesirably increase the threshold current density. Knowing the proportionality between the parasitic current density and the parasitic coupling (anticrossing), one may devise a design that reduces this anticrossing and hence the parasitic current density which in turn reduces the threshold current density. One way to implement this is to separate the injector state from the lower parasitic states spatially, as performed in the diagonal design of [2], which was pointed out earlier in Section 1. Modifying this diagonal design, we have reduced the anticrossing almost 50% of the value reported by [2]. Furthermore, by devising a strategy we have detuned the lower laser state from the upper collector state, which in turn, has reduced the QCL gain linewidth. Fig. 1(a), illustrates the conduction band diagram of the QCL under the design bias of 13.6 kV/cm at which the injector level (1′) and the upper laser level (4) are in resonance. The operating temperature is assumed to be T=5 °K. The module consists of an $Al_{0.17}Ga_{0.83}As/Al_{0.03}Ga_{0.97}As/GaAs/Al_{0.15}Ga_{0.85}As/Al_{0.01}Ga_{0.99}As/Al_{0.15}Ga_{0.85}As/GaAs/Al_{0.03}Ga_{0.97}As$ material system. As observed in Fig. 1(a), under the operating bias a diagonal radiative transition of frequency $f \approx E_{43}/h \approx 4.3$ THz occurs from 4→3, while levels 3 and 2 are in coherent resonance tunneling. Note that h is the Planck′s constant. The collector level population, under goes a nonradiative depopulation process to level 1 that acts as the injector level to the next module. Energy of the nonradiative transition is absorbed by a longitudinal optical (LO) phonon of the same energy (i.e., E_{21}=37.7 meV) in GaAs. Also seen in this figure are the extended wavefunctions for states 1′ and 4 with an energy splitting (injector anticrossing coupling) of $\Delta_{1'4}$=1.43 meV.

Figure 1(b) shows the QCL conduction band under the parasitic bias of 9.04kV/cm at which level 1′ from the preceding module is in resonance with the upper collector level (2) in the next module with anticrossing coupling of $\Delta_{1'2}$=0.29 meV. This has resulted in a parasitic current channel due to LO phonon scattering from level 2 to 1.

Iranian Journal of Electrical & Electronic Engineering, 2011.
Paper first received 4 Dec. 2010 and in revised form 4 Jan. 2011.
* The Author is with the Department of Electrical and Computer Engineering, Advanced Device Simulation Lab (ADSL), Tarbiat Modares University, P. O. Box 14115-143, Tehran 1411713116, Iran.
E-mails: farshi_k@modares.ac.ir, f_esmailifard@modares.ac.ir.
** The Author is with the School of Engineering, Shahed University, P.O. Box 18155-159, Tehran, Iran.
E-mail: saghafik@shahed.ac.ir.

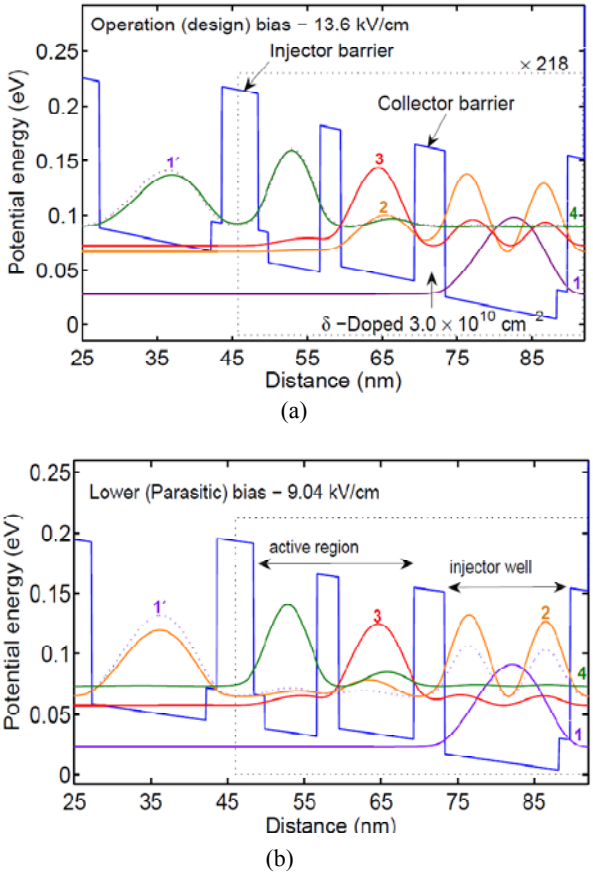

Fig. 1 Conduction band of the three-well active module with the squared magnitude of the envelope wavefunctions obtained by the extended Hamiltonian approximation under (a) the operating bias of 13.6 kV/cm, and (b) a lower parasitic bias of 9.04 kV/cm, as characterized by the 1′→4 and 1′→2 alignments, respectively.

It is well known that, in a THz-QCL, the stronger the injector anticrossing the broader the gain spectrum is. In order to minimize the broadening effect, one needs to maintain the injector anticrossing in the range of $1.4\ \text{meV} < \Delta_{1'4}^{\text{opt}} < 1.5\ \text{meV}$ [4]– i.e., the optimized injector anticrossing.

However, the injector, the collector, and the parasitic anticrossings that can be calculated for the three-well THz-QCL with diagonal transition fabricated by [2], as the reference points for comparison, are: $\Delta_{1'4}^{\text{ref}} \approx 2.23\ \text{meV}$, $\Delta_{32}^{\text{ref}} \approx 5\ \text{meV}$, $\Delta_{1'2}^{\text{ref}} \approx 0.54\ \text{meV}$ and dipole matrix element $z_{43}^{\text{ref}} \approx 3.7\ \text{nm}$ .The superscript "ref" is to indicate the reference. In order to approach the optimized range, one may increase either the injector barrier height or width from the reference values. In the present design, in order to approach $\Delta_{1'4}$, and also keeping the parasitic anticrossing as low as possible, we have combined both techniques. As shown in Fig. 1, in addition to increase the injector barrier height by 18 meV (equivalent to an increase 2% in Al mole fraction), with respect to those of the other two barriers in the module, we have added two 5-monolayer step-barriers of $Al_{0.03}Ga_{0.97}As$, on both sides of the injector barrier.

Furthermore, in order to increase the tunneling current through the collector barrier, as far as possible, the resonant coupling between levels 3 and 2 should also be as large as possible. The typical value of the collector coupling, Δ_{32}, used in literature is in the range of 4 meV <Δ_{32}<5meV [4]. On the other hand, for Δ_{32}>2 meV, the optical gain linewidth experiences an additional undesirable broadening.

As results of modifications, so far, we have achieved $\Delta_{1'4}$=1.43 meV, Δ_{32}=4.94 meV, $\Delta_{1'2}$=0.29 meV, $\Delta_{1'3}$=0.38 meV and $z_{43} \approx 5.05\ \text{nm}$. Meanwhile, the energy detuning δ_{32} (between energy levels 3 and 2) and $\delta_{1'4}$ (between energy levels 1′ and 4) are ignorable (i.e., the same as that of [2] $\delta_{32}^{\text{ref}} = \delta_{1'4}^{\text{ref}} = 0$). Notices, that in our design the parasitic anticrossing $\Delta_{1'2}$ is reduced to half of the reference point. Hence, in the modified design, the parasitic current $J_{1'2}$ is about one fourth of that obtained the reference diagonal design of [2]. Because for weak parasitic coupling, $J_{1'2} \propto (\Delta_{1'2})^2$ [6].

In order to compensate for the undesirable broadening, caused by Δ_{32}=4.94 meV, one may increase the collector energy detuning, δ_{32}. In order to do that, we have raised the bottom of the second active well by about 8.9 meV. This is done by replacing the GaAs as the original well material used in [2] with $Al_{0.01}Ga_{0.99}As$. This has resulted in an energy detuning of δ_{32}=4.38 meV which is not much less than E_{43}=17.7 meV, as illustrated in Fig. 2(a).

In order to calculate the energy levels across the module, shown in this figure, we have used the tight-binding model for the resonant tunneling across the injector and the collector barriers. The integer number below each barrier/well layer indicates the number of monolayers forming that particular layer in the module. Each monolayer for this lattice matched system of materials is about 0.2825 nm. Using the energy levels and the wavefunctions illustrated in Fig. 2(a) we have calculated the radiative energy, E_{43}, and the nonradiative depopulating energy, E_{21}, versus the applied electric field. Figure 2(b) illustrates these variations in E_{43} and E_{21} versus the electric field. Also shown in this figure are the injector, collector and parasitic channels anticrossings ($\Delta_{1'4}$, Δ_{32}, $\Delta_{1'2}$, and $\Delta_{1'3}$) that have been extracted from the results of Fig. 1 with extended wavefunctions. As also seen in this figure, the operation (design) bias coincides with the bias (13.6 kV/cm) at which injector anticrossing of $\Delta_{1'4}$=1.43 meV with zero detuning ($\delta_{1'4}$=0) occurs.

To investigate the effect of injector anticrossing and collector detuning on gain spectra broadening, we demonstrate the numerical results for the gain spectra as illustrated in Fig. 3(a). As observed in this figure, the dashed line represents the gain for $\Delta_{1'4}$=1.43 meV,

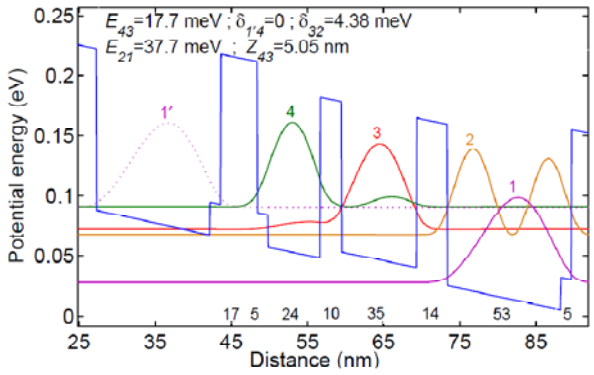

(a)

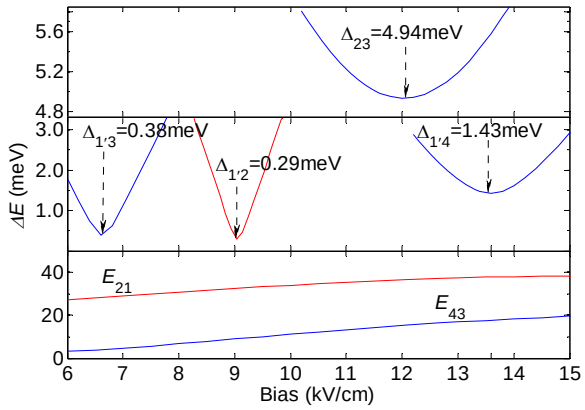

(b)

Fig. 2 (a) Conduction band of the three-well active module under the operating bias of 13.6 kV/cm, with the squared magnitude of the envelope wavefunctions obtained by the tight-binding approximation. (b) Anticrossings (calculated via extended Hamiltonian) and energy separations (obtained by tight-binding Hamiltonian), for the design.

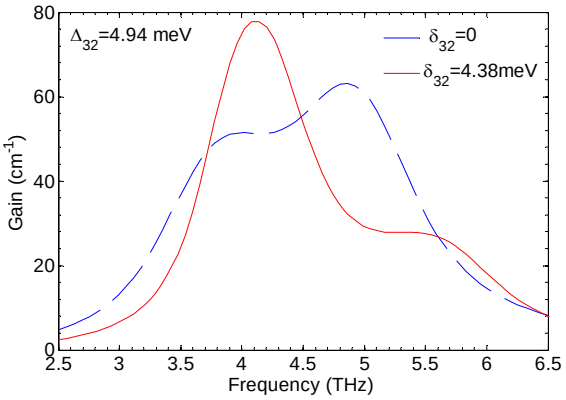

(a)

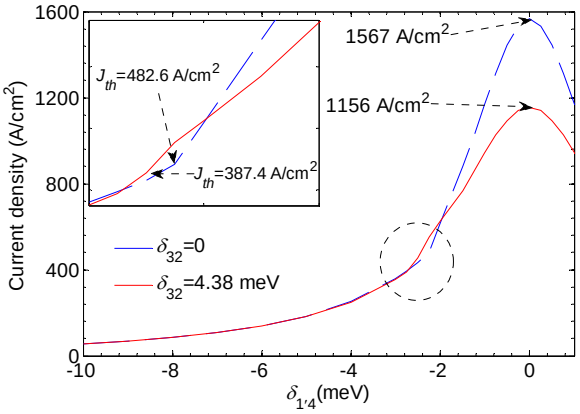

(b)

Fig. 3 (a) Optical gain for collector energy detuning of δ_{32}=0 (dashed-line) and δ_{32}=4.38 meV (solid line); (b) Steady state resonant tunneling current density through levels 1′ and 4 versus $\delta_{1'4}$.

Δ_{32}=4.94 meV, and δ_{32}=0. That gain full width at half maximum is FWHM =2.1 THz and peak gain is 63.1 cm^{-1}. For the final design in which the collector energy detuning is also increased to δ_{32}=4.38 meV, the line broadening is reduced to FWHM=1 THz, while, the peak gain is increased to 77.81 cm^{-1} that occurs at the frequency of f_{peak}=4.1 THz ($<E_{43}/h$). This shift in the frequency is due to the energy detuning (δ_{32}).

Moreover, to investigate the effect of the energy detuning (δ_{32}) on the steady state resonant-tunneling current through levels 1′ and 4, we have calculated the current density (J) versus $\delta_{1'4}$ (as illustrated in Fig. 3(b)). Note that $\delta_{1'4}$ is proportional to the external bias [4]. The dashed and solid lines represent the current densities corresponding to the cases illustrated by the dashed and solid lines in Fig. 3(a), respectively.

For calculating these two curves, we have included the electron-photon interaction as well as the injector and collector anticrossings. While in analytic method of [2] the electron-photon interaction was ignored.

When carriers are injected through the collector barrier by means of resonant tunneling, the lifetime of the lower laser level increases [4]. Also the electron-photon interaction beyond threshold reduces the lifetime of the upper laser level due to stimulated transitions. Both of these reduce the peak in the current density. Furthermore, the solid line demonstrates that when the collector detuning in the final design is increased to δ_{32}=4.38 meV, the peak in current intensity decreases further. This detuning increases the lifetime of the lower laser level, which in turn, decreases the FWHM of the frequency linewidth due to scattering decreases [4]. This reduction in FWHM also reduces the resulting threshold current intensity (demonstrated by the inset in Fig. 3(b)). Notice, as the frequency linewidth due to scattering becomes narrower; the required population inversion, required for the threshold gain, becomes smaller. As shown in Fig. 3(b), in the absence of the collector detuning (δ_{32}=0), J_{th}= 482.6 A/cm^2. Whereas, the threshold current for the final design, with δ_{32}=4.38 meV, is J_{th}= 387.4 A/cm^2 that occurs at a smaller $\delta_{1'4}$. From Fig. 3(b), one can realize that the maximum current density J_{max} and the dynamic range for lasing (J_{max}/J_{th}) for the final design (with $\Delta_{1'4}$=1.43 meV and δ_{32}=4.38 meV) are both reduced. On the other hand Fig. 3(a) shows that the laser gain is increased by 23.3%.

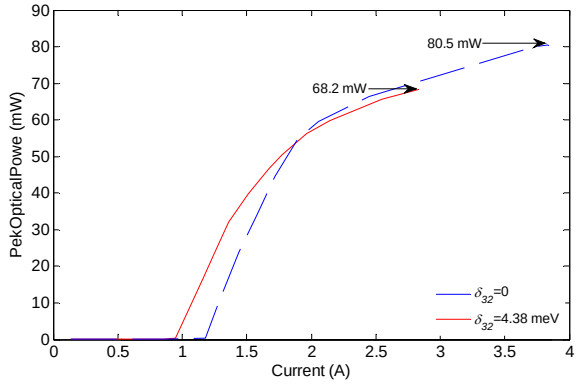

Fig. 4 Peak optical power versus current for different energy detuning of δ_{32}=0 (dashed-line) and δ_{32}=4.38 meV (solid line).

Figure 4 illustrates the peak power for the final design versus the device current (solid line). The device top contact geometry is assumed to be the same as that used by [2] with cross-sectional area of A=2.448×10^{-3} cm^2 and the cavity mirror loss is taken to be α_m=4 cm^{-1}. The dashed line in this figure shows the peak power for the laser in absence of the collector detuning (δ_{32}=0). The values of the peak powers that correspond to the peak current densities are labeled on the graph. The comparison shows that the peak power for the final design is about 15% less than the case δ_{32}=0 Using the data presented in this figure, we have calculated the differential quantum efficiency is also calculated to be $\eta=(e/\hbar\omega)\cdot(dp_{out}/dI)$~ 4.2 and 4.9 photon/electron for the structures with δ_{32}=4.38 meV δ_{32}=0, respectively.

3 Conclusion

We have presented an optimized design with narrow radiative linewidth FWHM in the GaAs/AlGaAs material system at 4.1THz. The design shows a lower threshold current, higher peak gain, smaller parasitic current channels (i.e., 1′→2 and 1′→3), in comparison to those of the earlier design. As a result, the smaller parasitic current channels have provided a better injection selectivity for the 1′→4 tunneling in a diagonal design.

Acknowledgment

This work was supported in part by Iran Telecommunication Research Center (ITRC) under Grant T-500-10312.

References

[1] Luo H., Laframboise S. R., Wasilewski Z. R., Aers G. C. and Liu H. C., "Terahertz quantum-cascade lasers based on a three-well active module", *Appl. Phys. Lett.*, Vol. 90, No. 4, pp. 041112–041114, 2007.

[2] Kumar S., Hu Q. and Reno J. L., "186 K operation of terahertz quantum-cascade lasers based on a diagonal design", *Appl. Phys. Lett.*, Vol. 94, No. 13, pp. 131105–131107, 2009.

[3] Scalari G., Amanti M. I., Fischer M., Terazzi R., Walther C., Beck M. and Faist J., "Step well quantum-cascade laser emitting at 3 THz", *Appl. Phys. Lett.*, Vol. 94, No. 4, pp. 041114–041116, 2009.

[4] Kumar S. and Hu Q., "Coherence of resonant-tunneling transport in terahertz quantum-cascade lasers", *Phys. Rev. B*, Vol. 80, pp. 245316-245329, 2009.

[5] Kumar S., Williams B. S. and Hu Q., "1.9 THz quantum cascade lasers with one-well injector", *Appl. Phys. Lett.*, Vol. 88, No. 12, pp. 121123-121125, 2006.

[6] Sirtori C., Capasso F. and Faist J., Hutchinson A. L., Sivco D.L. and Cho A. Y., "Resonant tunneling in quantum cascade lasers", *IEEE J. Quantum Electronics*, Vol. 34, No. 9, pp. 1722-1729, Sep. 1998.

Farnoush Esmailifard was born in Tehran, Iran, in 1976. She received the BSc degree in electrical engineering from Semnan University, Iran in 1999, and the M.S. degree from the Iran University of Science and Technology, Tehran, Iran, in 2002. She is currently working toward the Ph.D. degree in Advanced Device Simulation Lab (ADSL), Department of Electrical and Computer Engineering, Tarbiat Modares University, Tehran, Iran. Her research interests are modeling and simulation of semiconductor optoelectronic devices, and semiconductor quantum lasers.

Mohammad Kazem Moravvej-Farshi was born in Yazd, Iran, in 1952. He received the B. Sc. and the M. A. degrees in physics from Sharif University of Technology (SUT), Tehran, Iran, in 1976, and the University of Southern California (USC), Los Angeles, California, in 1978, respectively, the M. Sc. and the Ph. D degrees in electronics from the University of California at Santa Barbara (UCSB), in 1980, and the University of New South Wales (UNSW), Sydney, Australia, in 1987, respectively. From 1980 to 1984, he was a member of research staff with the Division of Microwave, Iran Telecommunication Research Center (ITRC). He joined Tarbiat Modares University (TMU) in 1987, where he is currently a Professor of Electronics and head of the Advanced Device Simulation Lab (ADSL). His current fields of interest are Avalanche Photo Diodes; All-optical devices based on Photonic Crystals and nanostructures; Nanophotonics; and Nanoelectronic Devices based Carbon nanotubes and Graphene nanoribbons. He has translated from English to Farsi four books in the field of semiconductor devices and one in laser electronics. His last translation in 2004 was selected as the best translation of the year in the field of engineering and applied sciences. M. K. Moravvej-Farshi was elected as one of the two most prominent professors of 2002 in the field of electrical engineering, nationwide. Professor Moravvej Farshi

is currently a senior member of IEEE, and also a senior member of Optical Society of America (OSA). He is also one of the founders of the Optics and Photonics Society of Iran (OPSI). He has been elected IEEE Iran Section Vice president for the period 2009-2011.

Kamyar Saghafi was born in Tehran, Iran, on December 19, 1963. He received the B. Sc. degree in electrical engineering from Iran University of Science and Technology in 1991, and the M. Sc. degree and Ph.D. degree in electrical engineering both from Tarbiat Modares University, Iran, in 1994 and in 1999, respectively. He joined the department of Electrical Engineering of Shahed University, Iran, in 1999. He has been working on simulation of submicron semiconductor devices. His current research interests are centered on the physics of nanoelectronic and optoelectronic devices. He is presently working on numerical modeling and simulation of nano devices such as carbon nanotube field effect transistors, single electron transistors and nanowire transistors.